Do Molecular Conductances Correlate with Electrochemical Rate Constants? Experimental Insights

10 AUTHORS, INCLUDING:

Xiao-Shun Zhou
Zhejiang Normal University
31 PUBLICATIONS **1,261** CITATIONS

SEE PROFILE

Noureddine Raouafi
University of Tunis El Manar
56 PUBLICATIONS **191** CITATIONS

SEE PROFILE

Bernd Schöllhorn
Paris Diderot University
81 PUBLICATIONS **1,087** CITATIONS

SEE PROFILE

Do Molecular Conductances Correlate with Electrochemical Rate Constants? Experimental Insights

Xiao-Shun Zhou,[∇,†,‡,§] Ling Liu,[∇,‡] Philippe Fortgang,[§] Anne-Sophie Lefevre,[§] Anna Serra-Muns,[§] Noureddine Raouafi,[§,⊥] Christian Amatore,*,[§] Bing-Wei Mao,*,[‡] Emmanuel Maisonhaute,*,[§,¶] and Bernd Schöllhorn*,[§,#]

[†]Zhejiang Key Laboratory for Reactive Chemistry on Solid Surfaces, Institute of Physical Chemistry, Zhejiang Normal University, Jinhua, Zhejiang 321004, China

[‡]Chemistry Department and State Key Laboratory for Physical Chemistry of Solid Surfaces, College of Chemistry and Chemical Engineering, Xiamen University, Xiamen 361005, China

[§]UMR CNRS 8640 Pasteur, Ecole Normale Supérieure, Université Pierre et Marie Curie — Paris 06, 24 rue Lhomond, 75231 Paris Cedex 05, France

[⊥]Laboratoire de Chimie Analytique et d'Electrochimie, Département de Chimie, Faculté des Sciences de Tunis, Université El-Manar, 2092 Tunis El-Manar, Tunisia

[¶]LISE-Laboratoire Interfaces et Systèmes Electrochimiques, UPR 15 du CNRS, Université Pierre et Marie Curie — Paris 06, Case Courrier no. 133, 4 place Jussieu, 75252 Paris Cedex 05, France

[#]Laboratoire d'Electrochimie Moléculaire, Université Paris Diderot — Paris 07, CNRS UMR 7591, 15 rue Jean-Antoine de Baïf, Bat. Lavoisier, 75013 Paris, France

S *Supporting Information*

ABSTRACT: We measured single-molecule conductances for three different redox systems self-assembled onto gold by the STMBJ method and compared them with electrochemical heterogeneous rate constants determined by ultrafast voltammetry. It was observed that fast systems indeed give higher conductance. Monotonous dependency of conductance on potential reveals that large molecular fluctuations prevent the molecular redox levels to lie in between the Fermi levels of the electrodes in the nanogap configuration. Electronic coupling factors for both experimental approaches were therefore evaluated based on the superexchange mechanism theory. The results suggest that coupling is surprisingly on the same order of magnitude or even larger in conductance measurements whereas electron transfer occurs on larger distances than in transient electrochemistry.
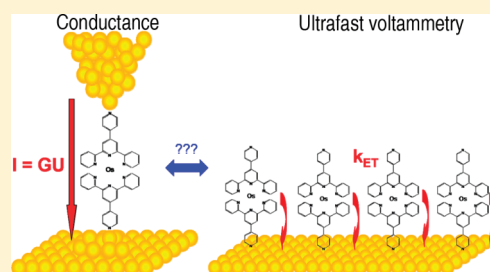
1. INTRODUCTION

Evaluation of electron transport properties of molecular structures is under increasing focus, the aim being to provide not only guidance for building efficient signal transduction for future bottom-up devices[1,2] but also to enable deeper insight into chemical/electrochemical processes. Several experimental approaches are relevant in this field. Among them, transient spectroscopy has proven to be useful to initiate electron transfer between an acceptor A and a donor D separated by a bridge in a molecule.[3,4] Electrochemical techniques that involve replacement of A or D by an electrode allow a current to be registered toward or from a redox center that is incorporated into the bridge.[5] Both of these types of techniques afford rate constants and thus kinetic parameters of thermalized electron transfer. Furthermore, though in voltammetry the method is statistical, being performed onto a large number of molecular systems, only a single electron per molecule is transferred, creating a permanent change in the molecule. Conversely, when both A and D are

replaced by electrodes, a steady-state current flows; hence, a conductivity through the bridge can be estimated. Development of the mechanically controllable break junction (MCBJ) technique or the scanning tunneling microscopy break junction (STMBJ) technique has presently reached the single-molecule limit[6−9] of molecular conductance determination in the junction.

Theoretical formulations relevant for the diverse experimental setups differ in the way the electronic and vibrational states are taken into account. For a molecular entity, there is generally a single electronic state to consider, but a continuous distribution of vibrational states is involved through the so-called Franck—Condon factor:

$$F = \frac{e^{-(\lambda + E_{AD})^2/4\lambda k_B T}}{\sqrt{4\pi\lambda k_B T}} \tag{1}$$

Scheme 1. Molecular Systems Considered in the Present Work
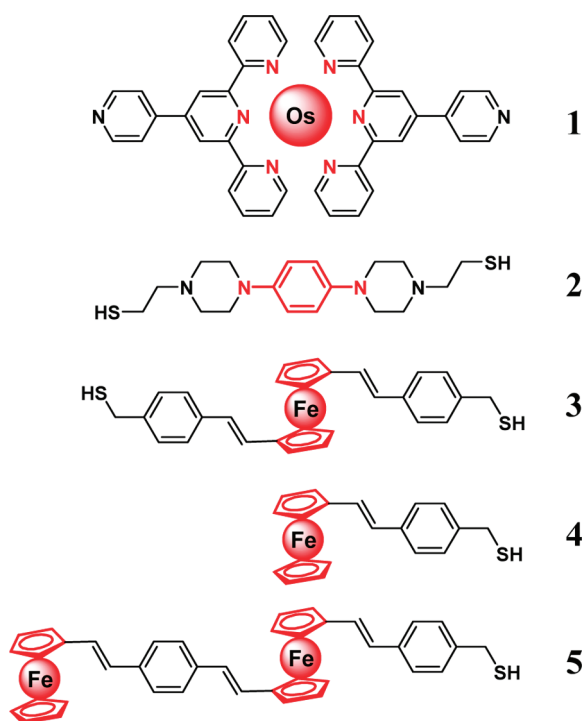
where λ is the reorganization energy of the redox center and E_{AD} the energy difference between donor and acceptor.[4] Conversely, for an electrode, the vibrational level influence can be neglected but electron transfer may occur from (or to) a Fermi–Dirac distribution of closely spaced energy levels. In all approaches, the parameter relevant to characterize the communication through the bridge is the electronic coupling factor H.[10]

In the case where a redox system is incorporated in the bridge itself, charge transport could become more complicated. Current modulation or rectification may depend on the redox state of the redox moiety.[11−16] In such a configuration, immersing the bridge into an electrolyte poised to a reference electrode allows the gating command to propagate through the solution. The reference electrode (i.e., the gate) can be placed far from the molecular junction under investigation. Therefore, only two conducting electrodes need to be arranged close enough to form a nanometric gap. However, mechanisms of charge transport would be complicated by fluctuations of solvent polarization and internal modes of the molecule.[17,18]

Our aim in this study was to contribute to the ongoing discussion about the relationship between conductivity and electron transfer rate constants in bridges equipped with a redox center. Indeed, though there is a formal equivalence, there is a big difference between communicating and localizing electrons or holes in a structure (as we do by our CV method) and simply passing charges through the structure by a tunnel effect favored by the quantum coupling within the structure (as in STMBJ). We thus selected the three very different molecules **1−3**, displayed in Scheme 1, with the aim of measuring both their molecular conductance using the STMBJ technique initially implemented by Tao et al.[7,19,20] and their heterogeneous rate constant by ultrafast cyclic voltammetry.[21] Molecules **1−3** differ widely in the

nature of their redox center, bridging unit, and metal-contacting atoms but have similar size (about 1.9 nm). Whereas it is relatively easy to measure molecular conductance when conductions are rather high, it is conversely more difficult to accurately determine fast electrochemical rate constants because ohmic losses in the solution filter the electrochemical information. We addressed this problem by the employment of microelectrodes with a specific potentiostat that allows compensation of ohmic losses with a sweep rate up to 2.5 megavolts per second in cyclic voltammetry. This setup is equivalent to a few tens of nanoseconds resolution[21−23] so that transient electrochemistry is now useful to investigate fast transduction which is obviously the most interesting domain for future practical applications of molecular electronic devices.

2. EXPERIMENTAL DETAILS

2.1. Synthesis. The detailed synthesis of compounds **1−3** is reported in the Supporting Information.

2.2. Adsorption Conditions. The adsorption conditions were optimized for each compound. For **1**, a gold single crystal was immersed into a CH$_3$CN solution of **1** (0.1 mM) for 5 min, and then for 10 min in the pure solvent. For **2**, the electrode was first immersed into a 0.05 mM CH$_2$Cl$_2$ solution of **2** for 1 h at 4 °C and then for 1−2 h in pure solvent after a thorough rinsing. The self-assembled monolayer of **3** was formed by soaking the electrode overnight in a chloroform solution containing 0.1 mM **3** and 0.1 mM pentanethiol 0.1, the latter being used as a diluent to minimize hairpin adsorption of **3** by both thiol functions on the surface (see below). After being thoroughly rinsed with chloroform, the electrode was immersed in pure chloroform for 2−4 h to remove physically adsorbed molecules.[24]

2.3. STM Experiment. Experiments for **1** and **2** were performed using an Agilent 5100 microscope. Gold tips were prepared electrochemically[25] and then insulated using Apiezon wax to obtain a leakage current of less than a few picoamps. A gold 111 crystal from Mateck was used for adsorbing the molecules. Prior to the STMBJ experiment, an image of the substrate was recorded to ensure that a single monolayer was obtained. Approach and retraction of the tip were performed using the custom spectroscopy mode in Picoscan 5.4. The tip was driven toward the surface, and then it was held at a constant distance for typically 200 ms in order to form some molecular junctions. Then the tip was retracted at a typical speed of 5 nm s^{-1}. The feedback was reestablished between each measurement.

Experiments with **3** were performed on a Nanoscope E STM (Veeco, Plainview, NY) modified to perform conductance measurements. Mechanically cut gold STM tips were used after insulation with thermosetting polyethylene glue for in situ STM measurements. Platinum wires were used as both counter- and quasireference electrodes. Voltammograms were recorded on a CHI potentiostat with an SCE reference electrode and a Pt counter electrode. All potentials for **3** are thus reported with respect to SCE.

Histograms were obtained by manual selection of conductance traces. Traces displaying monotonous decay or mechanical vibration were discarded. A parallel automatic analysis where conductance plateaus were evaluated numerically by calculation of the current standard deviation over a given interval gave similar results.

2.4. Ultrafast Cyclic Voltammetry. Ultrafast cyclic voltammetry was performed with a homemade potentiostat, allowing online compensation for ohmic losses.[22,23] Electron transfer rates were estimated from the peak displacement fitting using Laviron plots and supposing a transfer coefficient α of 0.5. The working, reference, and counter electrodes were lithographically produced Au band electrodes for **1**.[26] Since lower scan rates were necessary for **2**, gold balls could be used as

7510

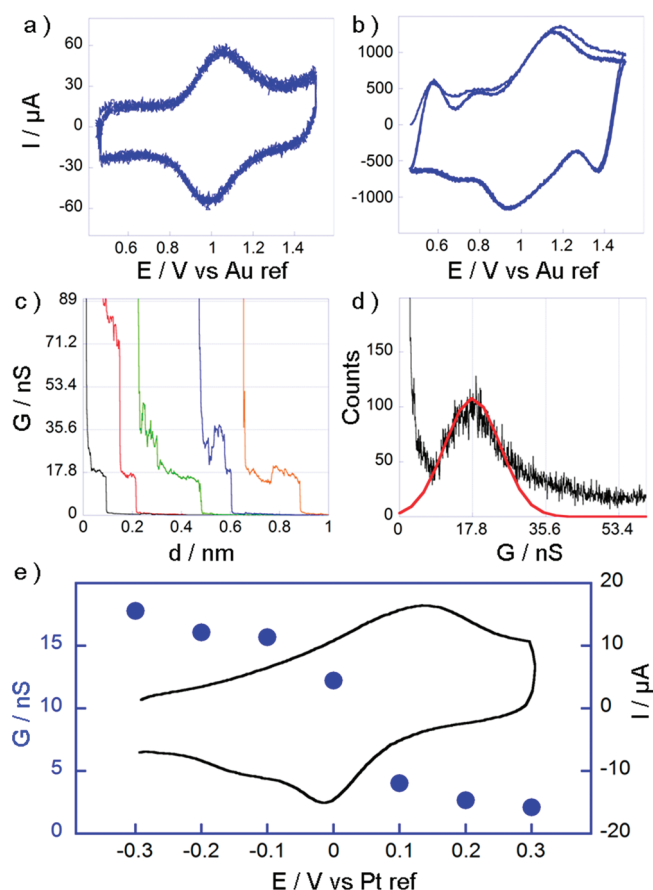dx.doi.org/10.1021/ja201042h |*J. Am. Chem. Soc.* 2011, 133, 7509–7516

Figure 1. Cyclic voltammograms of molecule **1** at (a) 10400 V s^{-1} and (b) 407000 V s^{-1}, three consecutive scans, no average. Electrolyte: H$_2$O + 1 M NaClO$_4$. (c) Some conductance traces obtained for **1** at a sample potential of −0.3 V/Pt and a bias of 50 mV. Electrolyte: 0.1 M NaClO$_4$ aqueous solution. (d) Histogram obtained from the selection of 211 out of 1000 conductance curves. (e) Filled circles: molecular conductance versus sample potential. Black line: cyclic voltammogram.

working electrodes. The reference was then an SCE, and Pt was used for the counter electrode.

3. RESULTS

3.1. Osmium Bisterpyridine. The first probe **1** was an osmium^{II} bisterpyridine complex that may be reversibly oxidized to Os^{III}. Figure 1a and 1b represents two voltammograms obtained for **1**. At "slow" scan rates, a voltammogram with bell-shape and almost symmetrical is obtained because equilibrium with the electrode is always sustained. At 407000 V s^{-1}, despite the very short time scale of the measurement, the peaks are only slightly shifted compared to their equilibrium position. However, this shift is significant and allows determination of the heterogeneous rate constant k_{ET} (see Supporting Information): $k_{ET} = 2.0 \times 10^6 \pm 0.5 \times 10^6$ s^{-1}. This value is smaller than the one determined by the same method for the complex Py(CH$_2$)$_2$-PyOsCl(bpy)$_2$ ($k_{ET} = 4 \times 10^6$ s^{-1}, Py standing for pyridine) by the same group[27] despite a shorter bridge length. This suggests that the reorganization energy for the Os(tpy)$_2$ redox center is probably higher than for PyOsCl(bpy)$_2$. Since the coordination sphere has nearly the same size, it is likely that the difference stems from a higher internal reorganization.

Molecular conductance was determined by the STMBJ method. Figure 1c displays typical stepwise current−distance curves for **1** at a sample potential of −0.3 V, thus within the stability region of Os^{II}. The bias voltage was fixed at 50 mV. Approximately 20% of the curves displayed detectable steps, which agrees with that reported in the literature.[6] The statistical analysis based on histogram construction displays a characteristic current peak which is attributed to the conductance current of a single-molecule junction (Figure 1d). While keeping the sample potential at −0.3 V, we varied the applied bias voltage from 10 to 200 mV. The conductance remained constant, confirming the reliability of our setup (see Figure S3 in Supporting Information).

The dependence of Au−**1**−Au junction conductance on the potential is reported in Figure 1e. We varied the sample potential from −0.3 to 0.3 V while the bias remained fixed at 50 mV. A cyclic voltammogram obtained on the Au(111) single crystal used to perform STMBJ measurements is also displayed in Figure 1e for comparison. There was a clear modulation of the conductance by the redox switching from 17.8 nS at −0.3 V to 2.1 nS at +0.3 V, which provides an on−off ratio of 8.5.

3.2. Phenylenediaminebisthiol. System **2** conversely contains saturated parts in the bridges, so that the redox center is better isolated from the electrodes. As a consequence, the rate of electron transfer is much slower: 7×10^4 s^{-1}. Since the resistance was higher, we observed more noise in the conductance curves, and it was more difficult but nevertheless possible to observe well-defined steps as depicted in Figure 2a. This allows the determination of a molecular conductance from the histogram presented in Figure 2b. From the resulting histograms constructed at different potentials (see Figure 2c), we deduced that the conductance shifts from 0.79 nS in the reduced state to 0.33 nS in the oxidized one. Modulation by the potential is thus smaller than for **1** but still appreciable (see Discussion). In the case of gold−sulfur bonds, reports of so-called "low" and "high" conductivity peaks (LC and HC) have often been observed in the literature. The common explanation is that the molecular conductivity depends strongly on the contact configuration, i.e., on the position of the sulfur atom on the electrode.[19,28,29] Tao initially proposed that when the sulfur is on a hollow site between three gold atoms, the conductivity is higher than when it stands on top of a single gold atom. On the other hand, bridge−bridge geometry has been predicted by Wandlowski to give the higher conductivity.[29] More recently, further studies by the Nichols group evidenced multiple sets of conductance values caused by the contact morphology, thus the atomic structure of the substrate surface.[30] The ratio HC/LC is usually around 5. We also observed a switch in the low conductance, with a shift from 0.13 to 0.09 nS (see Supporting Information).

3.3. Ferrocenebisthiol. Our attempts to perform experiments with monolayers formed from a solution of **3** alone did not provide enough curves with clear steps. Therefore, the resulting histograms did not display clear maxima so that the molecular conductance could not be properly evaluated. We assign these complications to the fact that rotation of the cyclopentadienyl rings around the iron possesses a low activation barrier, thus allowing anchoring of the molecule onto the surface with both thiol functions, which prevents single-molecule contacts. In order to avoid this problem, we coadsorbed pentanethiol to **3**. The resulting cyclic voltammograms of a Au(111) electrode modified with a mixture of **3** and pentanethiol are given in Figure 3a. A well-defined couple of redox peaks is present with a peak potential at 0.22 V vs SCE.
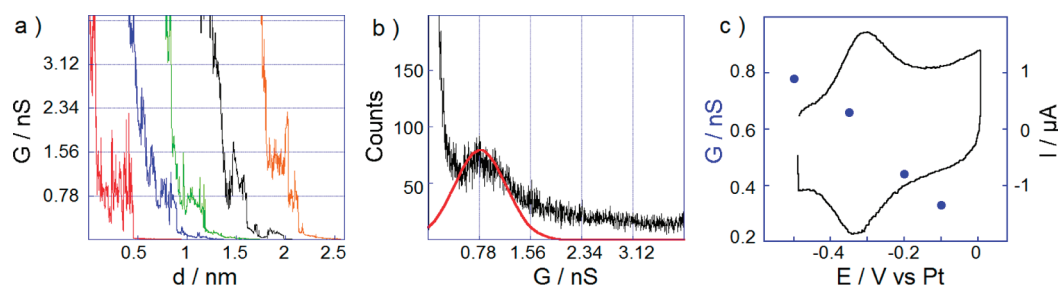
Figure 2. (a) Some conductance traces obtained at a sample potential of −500 mV and a bias of 100 mV for **2**. (b) Histograms at a sample potential of −500 mV. 165 out of 1000 curves were selected. (c) Filled circles: conductance as a function of electrode potential (left y axis). Black line: cyclic voltamogram of **2** (right y axis). Electrolyte: 0.1 M tetraethylammonium tetrafluoroborate aqueous solution.
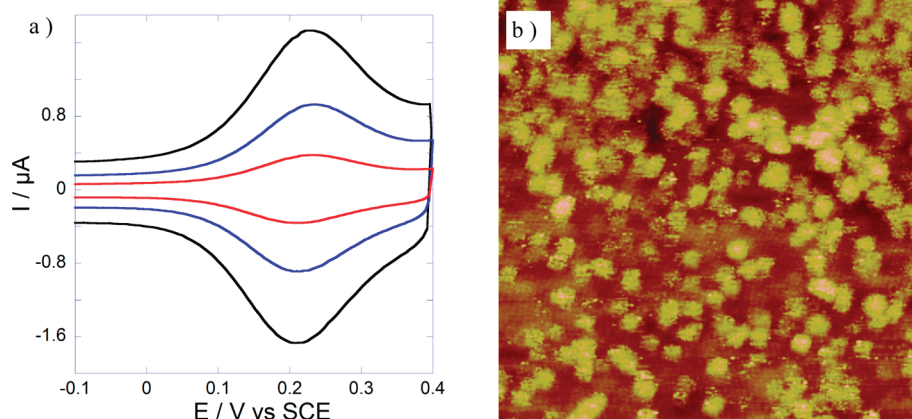

Figure 3. (a) Cyclic voltamograms of **3** coadsorbed with pentanethiol (see text) at 0.02, 0.05, and 0.1 V s^{-1} in H$_2$O + 0.1 M HClO$_4$. (b) Topography of mixed SAMs of **3** and C$_5$H$_{11}$SH adsorbed on Au(111) in 0.1 M HClO$_4$ solution at a substrate potential of 0.2 V (100 nm × 100 nm), I_t = 15 pA, bias = −0.1 V, Z-scale = 1 nm).

Figure 3b shows the STM image of the mixed SAM surface. The STM image is composed of big bright spots of diameter 4 to 6 nm ascribed to **3** on a relatively darker background attributed to the underlying pentanethiol monolayer for which molecular resolution is achieved. Several effects may explain the large diameter of the spots. First, similar to that proposed by Tour,[31−33] the bright spot corresponds to the tip structure imaged by the protruding redox molecules so that the size of the spot is not representative of the size of the molecule. Second, since the molecule in our system is less diluted than in Tour's work, single molecules are not always resolved, and the bright spots may correspond to molecular aggregates of the redox molecules alone or with the pentanethiol diluent. However, the nearly ideal voltametric response demonstrates that interactions between electroactive entities are minimal, suggesting that pentanethiol is likely inserted in the aggregate. More importantly, single-molecule junctions would anyway be formed in the final stage upon tip withdrawl regardless of the original number of molecules present in the aggregates (see below). Third, rotation over the Cp ring to get a twisted conformation would also enlarge the apparent diameter. The height and diameter of the spots remained unchanged upon potential variation from reduced (−0.1 V) to oxidized state (0.4 V) which serves as the first indication of possible conductance invariance with potential (see below).

Under these conditions, single-molecule conductance was measured at reduced (−0.1 V), oxidized (+0.4 V), and

intermediate (+0.2 V) redox states of **3** which forms mixed SAM with pentanethiol. This presents the advantage to prevent a looping around the cyclopentadienyl ring that could allow an anchoring with both thiols onto the electrode. As can be seen in Figure 4, clear steps could be observed, allowing histogram construction for either high or low conductance. Very surprisingly, the molecular conductance remained almost unchanged with potential, at a value close to 9.4 nS for HC and 2 nS for LC. The slight decrease observed near the standard potential (9.2 and 1.9 nS) is within the experimental error. The high conductivity is in agreement with the one determined previously in a MCBJ experiment without potential control (9.7 nS).[34] The conductance invariance observed for **3** severely contrasts with the behavior of systems **1** and **2** and with any other redox molecules that have been reported so far. Moreover, in some cases, we observed large fluctuations in the current while retracting the tip (see Figure 5a). This prompted us to stop the tip movement at a defined current close to high or low conductance and monitor the current as a function of time. Interestingly, discrete conductance switching around HC or LC was observed, two typical examples being displayed in Figure 5b and 5c. This subtle behavior is not directly apparent in the conductance histograms except for broadening of the histograms. Since it occurs for both HC and LC, it cannot be attributed to the contact geometry but rather to a conformational change of the molecule that induces a change in electronic coupling. Recently, it has been demonstrated that a direct contact between the tip and an aromatic ring

could be obtained.[30,35,36] However, it was also demonstrated that whenever adsorption by both thiols is possible, conductance peaks in the histograms are dominated by Au−S−molecule−S−Au configuration. Observation of HC and LC conductance peaks also confirms that **3** is linked by both thiols to the electrode, which seems plausible considering that the Au−S interaction is stronger than the Au-Cp one. At the present stage, it is impossible to identify the precise molecular changes responsible for these variations. Rotation of the cyclopentadienyl rings may be involved.

Our former ultrafast CV results for molecules **4** and **5** which possess a similar structure compared to **3** are very useful to relate with conductance measurements.[37] Very similar rate constants of ca. 5×10^6 s^{-1} for both **4** and **5** were obtained. In the case of **5**, a single two-electron wave was obtained, indicating that the singly oxidized intermediate was thermodynamically as well as kinetically unstable. The currently accepted explanation is that the positive charge is delocalized over the whole conjugated body and thus cannot be stabilized by the solvent.[38] Conversely, the charges are localized in the doubly oxidized molecule, and solvation brings a stabilization that may overcompensate for the initial electrostatic repulsion, particularly in polar media. A dramatic mechanistic change was thus observed when the intermediate redox center was buried inside a hydrophobic diluent. The almost independence of electronic coupling with the molecular length confirmed that phenylenevinylenes are indeed very good candidates for building efficient molecular devices.[5] Hence, this family provides a relatively high conductance and very fast electron transfers.

4. DISCUSSION

For electrochemical systems, theories have been developed to take into account the energy level variations inside the gap when the redox reaction occurs and different limiting situations may be encountered. Initially, Schmickler and co-workers evaluated the case of resonant tunneling when the oxidized or reduced level of the redox center has an energy level comparable with that of the electrodes.[39] This situation should in principle lead to a current maximum at potentials close to $E^0 \pm \lambda$ (E^0 is the standard potential) upon varying the sample potential. On the other hand, Ulstrup and co-workers have considered both reduced and oxidized states and electron hopping possibilities.[13,40−42] Upon electron transfer, the redox level relaxes to another equilibrium position. If coupling with the electrodes is very strong, several electron transfer events may occur during the relaxation. If the coupling is weak, relaxation occurs first, the electron is transferred to the second electrode, and relaxation toward the first equilibrium position ends the cycle. In adiabatic or nonadiabatic situations a conductance peak should thus be observed in the vicinity of the standard potential of the bridge. Influence of some experimental parameters is worth mentioning. First, the local potential at the redox site may be different because the potential drop is strongly affected by the tip potential. Second, the access of solvent molecules to the nanogap is restricted and the effective dielectric constant may differ, inducing a slower energy reorganization. Finally a conformational change may occur in the nanogap, hindering the resonance and leading to a so-called "soft gating" transition,[18,40,43] i.e., the one where a monotonous variation of the conductance is observed. This last point also
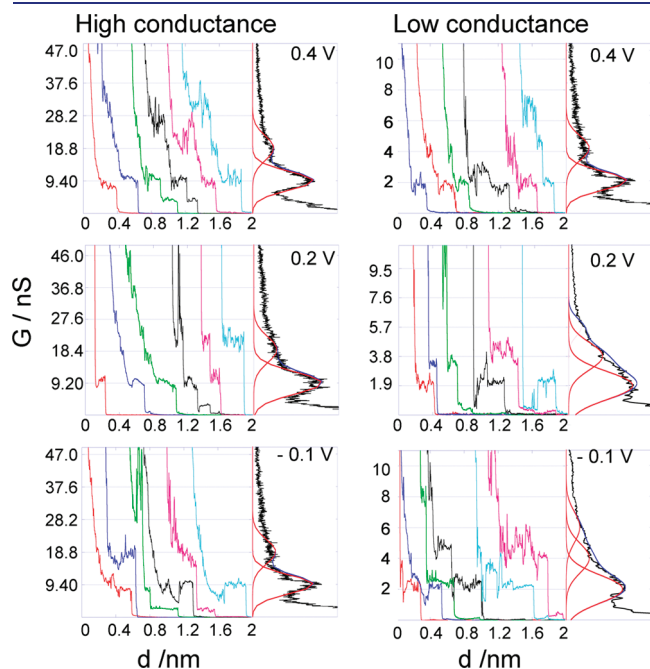

Figure 4. Typical conductance traces and histograms for high and low conductance at different potentials for molecule **3**. Potentials refer to SCE.
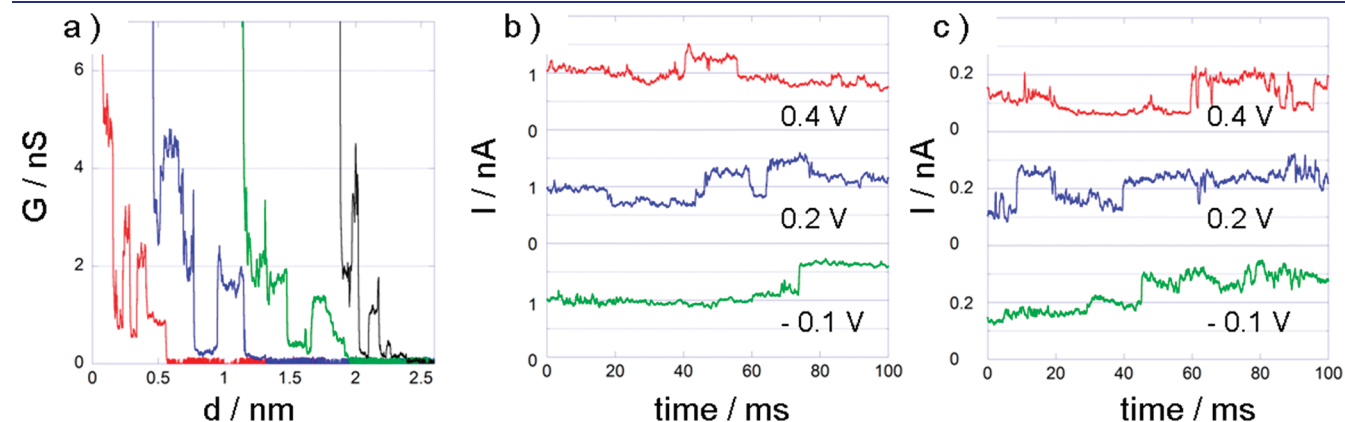

Figure 5. (a) Examples of stepwise conductance fluctuation shown in some conductance traces curves for low conductance. Sample potential 0.2 V vs SCE, bias: 100 mV for **3**. (b) Example of stepwise conductance fluctuations obtained by I−t measurements near the high conductance at different potentials. Bias: 100 mV. (c) Example of stepwise conductance fluctuations obtained by I−t measurements near the low conductance. Bias: 100 mV.
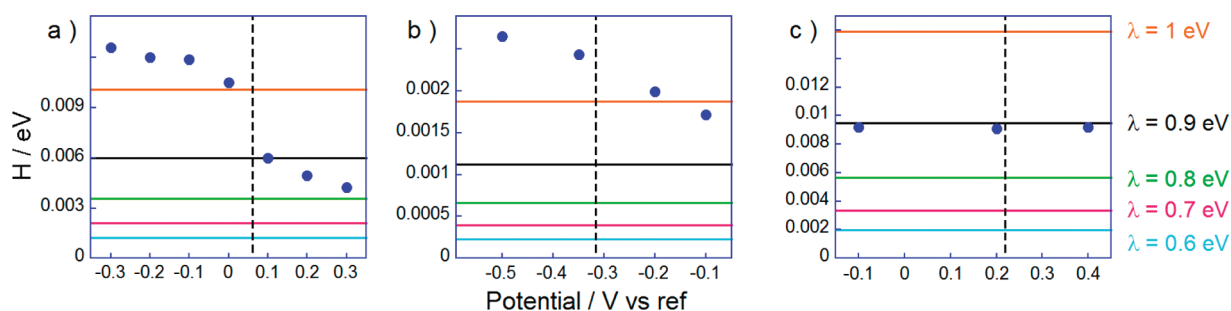
Figure 6. Estimated electronic coupling elements from conductance measurements (filled circles) and from ultrafast voltammetry (horizontal lines) for a range of reorganization energies ranging from 0.6 to 1 eV for **1** (a), **2** (b), and **3** (c). The vertical dashed line indicates standard potential. The potential scale refers to Pt for panels a and b, and to SCE for panel c.

depends on the precise experimental setup used to construct the nanogap since it may play a role in the local organization of the molecules inside the junction.

Experimentally, two different situations have been encountered in literature. The first class of systems is composed of electroactive self-assembled monolayers and investigated by tunneling spectroscopy. In this situation, many systems display a current maximum when the sample is poised near the standard potential. This is the case, for example, for a protoporphyrin,[44] several osmium and ferrocene complexes,[42,45,20] viologens,[46] and azurin, a redox protein.[47] The second category is composed of systems chemically anchored at both ends.[24,43,46,48,49] In that case, only the tetrathiofulvalenebisalkylthiol displayed a maximum.[43] For other systems of this category including ferrocenes or viologens, a monotonous variation of the conductance was observed. Perylenetetracarboxylic diimide derivatives displayed intermediate behavior.[16,48]

For our systems, the absence of any current maximum near the standard potential indicates a "soft-gating" mechanism, thus involving configurational dynamics of the molecule in the nanogap, as depicted by Ulstrup et al.[40,43] Electron transfer is assisted by the redox molecular levels that are not, however, in resonance with the Fermi levels of the electrode. Here, a potential variation modulates the coupling factor H_{conduc} but the mechanism continues to be a superexchange.[50,51] This demonstrates that large conformational fluctuations occur in the nanogap. It is noticeable that the larger on—off current ratio is higher for the more rigid system **1**. In the extending nanogap more degrees of freedom may be available for flexible molecules which would extend beyond the height of the diluent molecules, and the situation may thus greatly differ from the behavior in single-component types of self-assembled monolayers where the molecules are well-organized. In the framework of superexchange, theoretical equivalence between conductance measurements through a bridge and electron transfer from an electrode to a redox center separated from the electrode by the same bridge has been examined by several authors[4,52] and reinforce the intuitive idea that electron transfer rate constants should be correlated to single-molecule conductance.[53] From the Lewis formulation,[10,52] one deduces the following expressions for k_{ET} and G:

$$k_{ET} = \frac{2\pi^2}{h}\rho_M H_{ET}^2 \sqrt{\frac{\pi k_B T}{\lambda}} \times exp\left(-\frac{\lambda}{4k_B T}\right) \qquad (2)$$

$$G = \frac{4\pi^2 e^2}{h}H_{conduc}^2 \rho_M^2 \qquad (3)$$

where e is the elementary charge, and ρ_M is the electronic state density in the metal (supposedly identical in both electrodes). A currently accepted value for gold is $\rho_M = 0.27$ state eV^{-1}.[10,52] H_{ET} is the electronic coupling energy controlling the electron transfer rate constant and H_{conduc} imposes the conductance value.

The coupling factors H_{conduc} and H_{ET} were evaluated for a range of reasonable reorganization energies. For H_{conduc}, we resorted to the high conductance value since it is expected to be closer to the relaxed conformation of the SAM. Results are reported in Figure 6. For ferrocene and phenylene diamine derivatives λ is in the range 0.6—1 eV.[54—56] No reported λ value exists for **1**, but it may be expected to fall in the same range (see Supporting Information). Comparison of system **3** with **4** and **5** gives an excellent agreement ($H_{conduc} = 9.2 \times 10^{-3}$ eV ; $H_{ET} = 9.5 \times 10^{-3}$ eV) for $\lambda = 0.9$ eV, a very plausible value for ferrocenyl derivatives.[5,37] This may be correlated to the invariance of k_{ET} with the molecular length.[37] For **1** and **2**, H_{conduc} obtained at low potentials, therefore in the conformation for which the SAM is created, is clearly higher than H_{ET}. Since electron transfer operates over a longer distance in the conductance mode, this result is rather surprising, particularly for **2** whose redox center is connected through long saturated bridges. In the present study, we do not have a clear reference for the electrode—tip distance. For the conductance steps being observed within 0.2 nm, it is possible that while a step is observed, the molecule is in a stressed conformation, for example a partially folded or twisted one. Conversely, cyclic voltammetry is performed onto a relaxed geometry.[57—61] By temperature measurements of single-molecule conductance performed in air for dithioalkyls, Haiss et al. demonstrated that different high energy conformers indeed lead to higher conduction.[62] Conformational changes may be induced by the current itself,[63,64] or by the tip movement while or after the contact is established. A softer method to realize the contact could minimize the molecular fluctuations and lead to a better correlation.[8] Other recent evolutions of the STMBJ technique may also enable analysis and help to resolve this issue by allowing conductance measurements at various nanogap widths (i.e., at different molecular conformations).[8,65] These results, and particularly those for **3**, although showing a qualitative correlation between k_{ET} and G, highlight the need for further theoretical and experimental insights to fully understand the performances of complex molecular systems. These results also emphasize the need for independent and complementary experimental methods to estimate the device possibilities.

5. CONCLUSIONS

Molecular conductance and heterogeneous rate constants were evaluated for three molecular systems. Qualitatively, it was observed that fast electron transfer rate constants correspond to rather high conductances. Conductance variation with the potential suggests that superexchange, not electron hopping, is the predominate mechanism for the investigated molecules. The almost fully conjugated ferrocenebisthiol **3** even displayed a complete independence of conductance on potential when constructing histograms from $I-d$ curves. However, slight flips of conductance ascribable to conformational changes were observed when the tip movement was stopped after establishing an otherwise stable molecular junction. Tentative evaluations of electronic coupling revealed that, except for compound **3**, this parameter is surprisingly higher for steady-state conductance measurements than for transient electron transfer albeit the charge had to travel over a larger distance in the former case. This emphasizes that information derived from molecular structures should be evaluated through various experimental and theoretical approaches to elucidate intrinsic molecular complexity.

ASSOCIATED CONTENT

S **Supporting Information.** Reorganization energy evaluation of molecule **1**, additional data for conductance measurement and ultrafast cyclic voltammetry, synthesis of molecules **1**−**3**. This material is available free of charge via the Internet at http://pubs.acs.org.

AUTHOR INFORMATION

Corresponding Author

emmanuel.maisonhaute@upmc.fr; bwmao@xmu.edu.cn; christian.amatore@ens.fr; bernd.schollhorn@univ-paris-diderot.fr

Author Contributions

$^{\triangledown}$These two authors contributed equally to this work.

ACKNOWLEDGMENT

REFERENCES

(1) Ratner, M. *Nature* **2005**, *435*, 575.

(2) Joachim, C.; Ratner, M. A. *Proc. Natl. Acad. Sci. U.S.A.* **2005**, *102*, 8801.

(3) Nitzan, A. *Annu. Rev. Phys. Chem.* **2001**, *52*, 681.

(4) Nitzan, A. *J. Phys. Chem. A* **2001**, *105*, 2677.

(5) Sikes, H. D.; Smalley, J. F.; Dudek, S. P.; Cook, A. R.; Newton, M. D.; Chidsey, C. E. D.; Feldberg, S. W. *Science* **2001**, *291*, 1519.

(6) Chen, F.; Tao, N. J. *Acc. Chem. Res.* **2009**, *42*, 429.

(7) Xu, B. Q.; Tao, N. J. *Science* **2003**, *301*, 1221.

(8) Nichols, R. J.; Haiss, W.; Higgins, S. J.; Leary, E.; Martin, S.; Bethell, D. *Phys. Chem. Chem. Phys.* **2010**, *12*, 2801.

(9) Tian, J. H.; Yang, Y.; Liu, B.; Schollhorn, B.; Wu, D. Y.; Maisonhaute, E.; Muns, A. S.; Chen, Y.; Amatore, C.; Tao, N. J.; Tian, Z. Q. *Nanotechnology* **2010**, *21*, 274012.

(10) Traub, M. C.; Brunschwig, B. S.; Lewis, N. S. *J. Phys. Chem. B* **2007**, *111*, 6676.

(11) Yeganeh, S.; Galperin, M.; Ratner, M. A. *J. Am. Chem. Soc.* **2007**, *129*, 13313.

(12) Galperin, M.; Ratner, M. A.; Nitzan, A. *Nano Lett.* **2005**, *5*, 125.

(13) Albrecht, T.; Guckian, A.; Ulstrup, J.; Vos, J. G. *Nano Lett.* **2005**, *5*, 1451.

(14) Diez-Perez, I.; Hihath, J.; Lee, Y.; Yu, L. P.; Adamska, L.; Kozhushner, M. A.; Oleynik, I. I.; Tao, N. J. *Nat. Chem.* **2009**, *1*, 635.

(15) Gittins, D. I.; Bethell, D.; Schiffrin, D. J.; Nichols, R. J. *Nature* **2000**, *408*, 67.

(16) Xu, B. Q.; Xiao, X. Y.; Yang, X. M.; Zang, L.; Tao, N. J. *J. Am. Chem. Soc.* **2005**, *127*, 2386.

(17) Galperin, M.; Ratner, M. A.; Nitzan, A.; Troisi, A. *Science* **2008**, *319*, 1056.

(18) Zhang, J. D.; Kuznetsov, A. M.; Medvedev, I. G.; Chi, Q. J.; Albrecht, T.; Jensen, P. S.; Ulstrup, J. *Chem. Rev.* **2008**, *108*, 2737.

(19) Zhou, X. S.; Chen, Z. B.; Liu, S. H.; Jin, S.; Liu, L.; Zhang, H. M.; Xie, Z. X.; Jiang, Y. B.; Mao, B. W. *J. Phys. Chem. C* **2008**, *112*, 3935.

(20) Li, Z. H.; Liu, Y. Q.; Mertens, S. F. L.; Pobelov, I. V.; Wandlowski, T. *J. Am. Chem. Soc.* **2010**, *132*, 8187.

(21) Amatore, C.; Maisonhaute, E. *Anal. Chem.* **2005**, *77*, 303A.

(22) Amatore, C.; Maisonhaute, E.; Simonneau, G. *Electrochem. Commun.* **2000**, *2*, 81.

(23) Amatore, C.; Maisonhaute, E.; Simonneau, G. *J. Electroanal. Chem.* **2000**, *486*, 141.

(24) Xiao, X. Y.; Brune, D.; He, J.; Lindsay, S.; Gorman, C. B.; Tao, N. J. *Chem. Phys.* **2006**, *326*, 138.

(25) Ren, B.; Picardi, G.; Pettinger, B. *Rev. Sci. Instrum.* **2004**, *75*, 837.

(26) Fortgang, P.; Amatore, C.; Maisonhaute, E.; Schollhorn, B. *Electrochem. Commun.* **2010**, *12*, 897.

(27) Amatore, C.; Bouret, Y.; Maisonhaute, E.; Abruna, H. D.; Goldsmith, J. I. *C. R. Chim.* **2003**, *6*, 99.

(28) Li, X. L.; He, J.; Hihath, J.; Xu, B. Q.; Lindsay, S. M.; Tao, N. J. *J. Am. Chem. Soc.* **2006**, *128*, 2135.

(29) Li, C.; Pobelov, I.; Wandlowski, T.; Bagrets, A.; Arnold, A.; Evers, F. *J. Am. Chem. Soc.* **2008**, *130*, 318.

(30) Haiss, W.; Martin, S.; Leary, E.; van Zalinge, H.; Higgins, S. J.; Bouffier, L.; Nichols, R. J. *J. Phys. Chem. C* **2009**, *113*, 5823.

(31) Moore, A. M.; Mantooth, B. A.; Donhauser, Z. J.; Yao, Y. X.; Tour, J. M.; Weiss, P. S. *J. Am. Chem. Soc.* **2007**, *129*, 10352.

(32) Cygan, M. T.; Dunbar, T. D.; Arnold, J. J.; Bumm, L. A.; Shedlock, N. F.; Burgin, T. P.; Jones, L.; Allara, D. L.; Tour, J. M.; Weiss, P. S. *J. Am. Chem. Soc.* **1998**, *120*, 2721.

(33) Bumm, L. A.; Arnold, J. J.; Cygan, M. T.; Dunbar, T. D.; Burgin, T. P.; Jones, L.; Allara, D. L.; Tour, J. M.; Weiss, P. S. *Science* **1996**, *271*, 1705.

(34) Tian, J. H.; Yang, Y.; Zhou, X. S.; Schollhorn, B.; Maisonhaute, E.; Chen, Z. B.; Yang, F. Z.; Chen, Y.; Amatore, C.; Mao, B. W.; Tian, Z. Q. *ChemPhysChem* **2010**, *11*, 2745.

(35) Martin, S.; Grace, I.; Bryce, M. R.; Wang, C. S.; Jitchati, R.; Batsanov, A. S.; Higgins, S. J.; Lambert, C. J.; Nichols, R. J. *J. Am. Chem. Soc.* **2010**, *132*, 9157.

(36) Schneebeli, S. T.; Kamenetska, M.; Cheng, Z.; Skouta, R.; Friesner, R. A.; Venkataraman, L.; breslow, R. *J. Am. Chem. Soc.* **2011**, *133*, 2136.

(37) Amatore, C.; Maisonhaute, E.; Schollhorn, B.; Wadhawan, J. *ChemPhysChem* **2007**, *8*, 1321.

(38) Hapiot, P. F.; Kispert, L. D.; Konovalov, V. V.; Saveant, J. M. *J. Am. Chem. Soc.* **2001**, *123*, 6669.

(39) Schmickler, W.; Tao, N. J. *Electrochim. Acta* **1997**, *42*, 2809.

(40) Haiss, W.; Albrecht, T.; van Zalinge, H.; Higgins, S. J.; Bethell, D.; Hobenreich, H.; Schiffrin, D. J.; Nichols, R. J.; Kuznetsov, A. M.; Zhang, J.; Chi, Q.; Ulstrup, J. *J. Phys. Chem. B* **2007**, *111*, 6703.

(41) Albrecht, T.; Moth-Poulsen, K.; Christensen, J. B.; Guckian, A.; Bjornholm, T.; Vos, J. G.; Ulstrup, J. *Faraday Discuss.* **2006**, *131*, 265.

(42) Albrecht, T.; Guckian, A.; Kuznetsov, A. M.; Vos, J. G.; Ulstrup, J. *J. Am. Chem. Soc.* **2006**, *128*, 17132.

(43) Leary, E.; Higgins, S. J.; van Zalinge, H.; Haiss, W.; Nichols, R. J.; Nygaard, S.; Jeppesen, J. O.; Ulstrup, J. *J. Am. Chem. Soc.* **2008**, *130*, 12204.

(44) Tao, N. J.; Cardenas, G.; Cunha, F.; Shi, Z. *Langmuir* **1995**, *11*, 4445.

(45) Ricci, A. M.; Calvo, E. J.; Martin, S.; Nichols, R. J. *J. Am. Chem. Soc.* **2010**, *132*, 2494.

(46) Pobelov, I. V.; Li, Z. H.; Wandlowski, T. *J. Am. Chem. Soc.* **2008**, *130*, 16045.

(47) Chi, Q. J.; Farver, O.; Ulstrup, J. *Proc. Natl. Acad. Sci. U.S.A.* **2005**, *102*, 16203.

(48) Li, X. L.; Hihath, J.; Chen, F.; Masuda, T.; Zang, L.; Tao, N. J. *J. Am. Chem. Soc.* **2007**, *129*, 11535.

(49) Li, C.; Mishchenko, A.; Li, Z.; Pobelov, I.; Wandlowski, T.; Li, X. Q.; Wurthner, F.; Bagrets, A.; Evers, F. *J. Phys.: Condens. Matter* **2008**, *20*, 374122.

(50) Potential dependence of electroinactive molecules is usually negligible, though a slight effect was observed for 4,4′-bipyridine.[51]

(51) Li, X. L.; Xu, B. Q.; Xiao, X. Y.; Yang, X. M.; Zang, L.; Tao, N. J. *Faraday Discuss.* **2006**, *131*, 111.

(52) Royea, W. J.; Fajardo, A. M.; Lewis, N. S. *J. Phys. Chem. B* **1997**, *101*, 11152.

(53) In the present experimental situation the bridge size is thus double that in the Lewis theoretical formulation.

(54) Nielson, R. M.; McManis, G. E.; Safford, L. K.; Weaver, M. J. *J. Phys. Chem.* **1989**, *93*, 2152.

(55) Nelsen, S. F.; Ramm, M. T.; Ismagilov, R. F.; Nagy, M. A.; Trieber, D. A.; Powell, D. R.; Chen, X.; Gengler, J. J.; Qu, Q. L.; Brandt, J. L.; Pladziewicz, J. R. *J. Am. Chem. Soc.* **1997**, *119*, 5900.

(56) Nelsen, S. F.; Ismagilov, R. F.; Gentile, K. E.; Nagy, M. A.; Tran, H. Q.; Qu, Q. L.; Halfen, D. T.; Odegard, A. L.; Pladziewicz, J. R. *J. Am. Chem. Soc.* **1998**, *120*, 8230.

(57) Basch, H.; Cohen, R.; Ratner, M. A. *Nano Lett.* **2005**, *5*, 1668.

(58) Vonlanthen, D.; Mishchenko, A.; Elbing, M.; Neuburger, M.; Wandlowski, T.; Mayor, M. *Angew. Chem., Int. Ed.* **2009**, *48*, 8886.

(59) Mishchenko, A.; Vonlanthen, D.; Meded, V.; Burkle, M.; Li, C.; Pobelov, I. V.; Bagrets, A.; Viljas, J. K.; Pauly, F.; Evers, F.; Mayor, M.; Wandlowski, T. *Nano Lett.* **2010**, *10*, 156.

(60) Park, Y. S.; Widawsky, J. R.; Kamenetska, M.; Steigerwald, M. L.; Hybertsen, M. S.; Nuckolls, C.; Venkataraman, L. *J. Am. Chem. Soc.* **2009**, *131*, 10820.

(61) Taniguchi, M.; Tsutsui, M.; Shoji, K.; Fujiwara, H.; Kawai, T. *J. Am. Chem. Soc.* **2009**, *131*, 14146.

(62) Haiss, W.; van Zalinge, H.; Bethell, D.; Ulstrup, J.; Schiffrin, D. J.; Nichols, R. J. *Faraday Discuss.* **2006**, *131*, 253.

(63) Huang, Z. F.; Xu, B. Q.; Chen, Y. C.; Di Ventra, M.; Tao, N. J. *Nano Lett.* **2006**, *6*, 1240.

(64) Kihira, Y.; Shimada, T.; Matsuo, Y.; Nakamura, E.; Hasegawa, T. *Nano Lett.* **2009**, *9*, 1442.

(65) Kamenetska, M.; Quek, S. Y.; Whalley, A. C.; Steigerwald, M. L.; Choi, H. J.; Louie, S. G.; Nuckolls, C.; Hybertsen, M. S.; Neaton, J. B.; Venkataraman, L. *J. Am. Chem. Soc.* **2010**, *132*, 6817.